journal of the mechanical behavior of biomedical materials 125 (2022) 104873

Contents lists available at ScienceDirect

Journal of the Mechanical Behavior of Biomedical Materials

journal homepage: www.elsevier.com/locate/jmbbm

Research Paper

Nutritionally induced nanoscale variations in spider silk structural and mechanical properties

Sean J. Blamires [a,*], Madeleine Nobbs [a], Jonas O. Wolff [b], Celine Heu [c]

[a] Evolution & Ecology Research Centre, School of Biological, Earth & Environmental Sciences E26, The University of New South Wales, Sydney, 2052, Australia
[b] Department of Biological Sciences, Macquarie University, Sydney, NSW, 2109, Australia
[c] Katharina Gaus Light Microscopy Facility, Mark Wainwright Analytical Centre, LG12, Lowy Cancer Research Centre C25, The University of New South Wales, Sydney, 2052, Australia

ARTICLE INFO

Keywords:
Atomic force microscopy
Contact
Nanoindentation
Physical properties
Skin-core
Structures
Spider major ampullate silk

ABSTRACT

Spider major ampullate (MA) silk is characterized by high strength and toughness and is adaptable across environments. Experiments depriving spiders of protein have enabled researchers to examine nutritionally induced changes in gene expression, protein structures, and bulk properties of MA silk. However, it has not been elucidated if it varies in a similar way at a nanoscale. Here we used Atomic Force Microscopy (AFM) to simultaneously examine the topographic, structural, and mechanical properties of silks spun by two species of spider, *Argiope keyserlingi* and *Latrodectus hasselti*, at a nanoscale when protein fed or deprived. We found height, a measure of localized width, to substantially vary across species and treatments. We also found that Young's modulus, which may be used as an estimate of localized stiffness, decreased with protein deprivation in both species' silk. Our results suggest that nanoscale skin-core structures of *A. keyserlingi*'s MA silk varied significantly across treatments, whereas only slight structural and functional variability was found for *L. hasselti*'s silk. These results largely agreed with examinations of the bulk properties of each species' silk. However, we could not directly attribute the decoupling between protein structures and bulk mechanics in *L. hasselti*'s silk to nanoscale features. Our results advance the understanding of processes inducing skin and core structural variations in spider silks at a nanoscale, which serves to enhance the prospect of developing biomimetic engineering programs.

1. Introduction

Spider webs function by absorbing the kinetic energy of intercepted prey. The constituent silks thus need to be mechanically adaptable to perform optimally across different environments and/or when different prey types are encountered (Lin et al., 1995; Blamires et al., 2013; Harmer et al., 2015; Blamires and Sellers, 2019). The silk shouldering the burden of dispersing the kinetic energy absorbed during impact in spider orb webs and cobwebs is major ampullate (MA) silk (Sensenig et al., 2012; Lintz and Scheibel, 2013; Harmer et al., 2015; Blamires and Sellers, 2019). This is accomplished by initial high silk stiffness followed by gradual deformation (Kohler and Vollrath, 1995; Du et al., 2011; Sensenig et al., 2012; Tarakanova and Buehler, 2012; Blamires and Sellers, 2019). The silk needs to strike a balance between being too compliant and too stiff if the kinetic energy of the impacting prey is to be optimally absorbed (Liu et al., 2005; Boutry and Blackledge, 2013; Blamires and Sellers, 2019). If the fibres are too compliant the web will collapse on impact. On the other hand, if they are too stiff the prey will be ejected off the web (Hudspeth et al., 2012).

MA silk is organized into a lipid-protein-glycoprotein skin covering a fibrous protein core (Papadopoulos et al., 2009; Blamires et al., 2017) that is composed of at least two fibril forming proteins (spidroins), major ampullate spidroin 1, (MaSp1), and major ampullate spidroin 2 (MaSp2). MaSp1 consists of repeating polyalanine amino acid motifs that combine to promote the formation of crystalline β–sheet nano-structures and contribute directly to the strength of bulk fibres (Parkhe et al., 1997; Blamires et al., 2017). MaSp2 is thought to consist of multiple proline-rich motifs that form into disordered type II β-turns and other nano-structures to promote the remarkable extensibility of the fibres (Du et al., 2011; Blamires et al., 2017).

Covariation between the bulk properties and the primary and secondary protein structures within skin and core crystalline and amorphous regions has been revealed in silkworm silk (Guo et al., 2018). Nonetheless, spider MA silk performs fundamentally differently than

* Corresponding author.
E-mail address: sean.blamires@unsw.edu.au (S.J. Blamires).

https://doi.org/10.1016/j.jmbbm.2021.104873
Received 1 May 2021; Received in revised form 24 September 2021; Accepted 30 September 2021
Available online 4 October 2021

silkworm silk, so warrants an independent assessment. Compared to silkworm silk, MA silk has a high extensibility, low stiffness, and becomes rubbery on contact with water (Guan et al., 2013; Blamires et al., 2017). Much of this behaviour can be explained by amino acid compositions, and the subsequent nano-structural arrangements within the skin and core (Bratzel and Beuhler, 2011; Paquet-Mercier et al., 2013; Craig et al., 2019, 2020).

That being said, linking bulk mechanical properties with nanostructures in the skin and core of individual silks is prohibitively difficult when measurements are made at different scales (Eisoldt et al., 2010; Lin et al., 2015; Blamires et al., 2017). Our incomplete knowledge of the interplay between protein structures and silk properties across species and environments, at nano-to bulk fibre scales, remains a hindrance toward achieving the engineering goal of synthesizing a recombinant biomimetic spider silk for practical applications (Lin et al., 2015; Wolff et al., 2017).

A useful way to experimentally test the influence of variability in primary and secondary structures on the bulk properties of MA silk is to provide spiders diets of different nutritional composition (e.g. high or low protein composition) prior to collecting their silk to assess their mechanical, amino acid compositional, and nano-structural properties (Blamires et al., 2015, 2018). Previous work (Blamires et al., 2018) used this approach with different web building spiders and found that broad changes in structure and alignment in the amorphous region affected the bulk mechanical properties in most of the spider's silks. In one species, *A. keyserlingi*, an increase in amorphous region alignment was coupled with a decreased crystallinity inducing greater extensibility in their silks when deprived of dietary protein. These changes predictably coincided with variations in the amino acid composition of the silk as a consequence of variation in the ratio of MaSp1 and MaSp2 expressed (Blamires et al., 2018). In the silk of the cobweb spider *L. hasselti*, however, the amorphous and crystalline structures and bulk mechanical properties were unaffected by protein deprivation despite significant shifts in MaSp1: MaSp2 expression (Blamires et al., 2018). Such results suggest that silk nanostructures and bulk properties might become decoupled from gene expression in certain instances. Nevertheless, for reasons stated above, we cannot be certain why or how this decoupling occurs until we examine the silks at the nanoscale.

Atomic force microscopy (AFM) is a technique that provides the functionality to simultaneously probe the mechanical and surface properties of materials at the nanoscale (Neubauer et al., 2013; Silva and Rech, 2013). Examples of its application to examine the skin and core structure and function of silk includes as a means to determine: (i) the region specific elastic moduli of chimeric spider silk fibres and films (Gomes et al., 2011), (ii) the surface topography and its contribution to local mechanical properties in synthetically spun silk fibres (Menezes et al., 2013), and (iii) the molecular detail of silkworm and glow worm silks to ascertain structure and function (Zhang et al., 2000; Piorkowski et al., 2021). These studies demonstrate that AFM can be a powerful method for simultaneously probing the structures and mechanical properties of silks at a nanoscale while extracting information about surface topography (Hansma and Hoh, 1994).

Here we performed AFM experiments to examine the nanoscale structural properties, thread surface features, and localized mechanical properties, of two spider's, *A. keyserlingi* and *L. hasselti*, silks when fed diets that were either high in protein or deprived of protein, and ascertained the relationships between these features and the bulk properties. We chose these two species because one (*A. keyserlingi*) is a species of orb web spider that produces MA silk that is known to co-vary in nano-structural and bulk mechanical properties when protein deprived. More significantly, these variations have been shown to conform with the proposition that they are a consequence of the underlying MaSp1: MaSp2 expression. On the other hand, *L. hasselti* is a species of cobweb spider whose MA silk displays little or no structural or mechanical property variation when protein deprived regardless of its MaSp1: MaSp2 expression (Blamires et al., 2016, 2018; Craig et al., 2019).

2. Materials and methods

2.1. Spider collection and pre-feeding

Ten mature female *A. keyserlingi* and *L. hasselti* were collected from similar urban habitats in eastern Sydney, New South Wales, Australia, and taken to the laboratory at the University of New South Wales for experimentation.

Upon collection we measured the spider's body length to the nearest ±0.1 mm using digital Vernier calipers (ISO 9001, ISO, Australia), and mass to the nearest ±0.001 g using an electronic balance (Ohaus Corp., Pine Brook, NY, USA). These measurements were used to make sure we only took individuals of similar mass to the laboratory. All of the spiders were placed in 115 mm (wide) x 45 mm (high) plastic circular containers with perforated wire mesh lids containing a 20 mm long slit cut into them using a Stanley knife to facilitate feeding using a 20 μl micropipette. We fed them 20 μl of a 30% w/v glucose solution (prepared according to Blamires et al., 2015, 2018) over five days to standardize their nutrient uptake and silk production. We then collected silk, as outlined by Blamires et al. (2018), to remove the silk stored in the major ampullate glands prior to experimentation. We reweighed the spiders after silking them to ensure they approximately retained their mass at capture. We noticed that one *A. keyserlingi* became emaciated, losing >50% of its body weight, so this individual was discarded.

2.2. Experiments and silk collection

We randomly divided the remaining 19 spiders (9 *A. keyserlingi* and 10 *L. hasselti*) into two groups and fed them either one of two solutions over 10 days: a protein solution (P) or protein deprived solution (N). The solutions and their method of delivery were identical to that described by Blamires et al. (2018). After completing the feeding experiment, we re-weighed all spiders to check that they had not lost significantly more than 20% of their initial mass during the experiment.

We then collected silk following procedures outlined by Blamires et al. (2018) when collecting for tensile testing. We collected, for each spider, six cardboard frames each containing part of a single silk thread of MA silk. We collected, for *A. keyerlingi*: 24 threads (6 threads x 4 individuals) for the P treatment, and 30 threads (6 threads x 5 individuals) for the N treatment, and for *L. hasselti*: 30 threads (6 threads x 5 individuals) for the P treatment, and 30 threads (6 threads x 5 individuals) for the N treatment. The silk threads were stuck to a microscope slide by adding a drop of super glue at the junction of the cardboard frame and the thread. After allowing 24 h for the glue to dry, the cardboard frames were cut away leaving only the thread stuck to the slide.

2.3. AFM procedures

The threads prepared above were subjected to Peak Force Tapping mode AFM using a Bruker Bioscope Catalyst™ Atomic Force Microscope (Bruker, USA). We used Bruker ScanAsyst fluid Silicon Nitride probes to image the thread properties using single nanoindentation measurements. The nominal tip radius was 20 nm and the tip half angle set at 18°. The resonance frequency varied from 120 to 180 k Hz. Data was acquired using Bruker Nanoscope software and analysed with the Bruker Nanoscope Analysis 8.15 program. Height and Young's modulus (YM) were estimated as described below.

The slides containing the silk threads were mounted onto a stage suspended on a TMC vibration isolation table (Technical Manufacturing Corporation, USA) with the heating insert set at 23 °C. The motorized stage of the AFM was mounted onto a Leica DMI 3000 B optical microscope (Leica Microsystems, Wetzler, Germany), equipped with a SDR Scientific camera, which allowed us to locate the silk samples. Initial searches for fibres under the optical microscopy revealed that, in most

cases, two silk fibres were present and aligned side-by-side (Fig. 1).

Before performing each scan, the AFM was calibrated as described by Heu et al. (2012). This enabled us to accurately determine the tip radius, which was necessary for estimating DMT modulus (Bhushan and Koinkar, 1994) and roughness (Hansma and Hoh, 1994). The deflection sensitivity of the probe was measured in air at room temperature by engaging the probe on an uncoated sapphire substrate. Spring constant of the probe was measured using the integrated thermal tune sweep away from the sapphire surface. The scan size was set at 10 μm and scan rate at 0.1 μm/s. The silk threads were imaged in Peak Force Quantitative Nanomechanical (PFQNM) mode with the ScanAsyst auto-control on, and the peak force set point set as 22.961 Nn across all images. Other experimentally estimated or nominated parameters were: samples per line = 256, peak force amplitude = 150 nm, peak force frequency = 1 kHz, lift height = 146 nm, and Poisson's ratio of the silk sample (σ_{13}) = 0.33 (Patil et al., 2014; Garcia, 2020).

Using the PFQNM mode allowed us to simultaneously capture images across a 10 μm length of thread and intermittent contact force curves, from which features such as deformation, topography, height, and YM were estimated as follows. Individual curves were processed using the Nanoscope Analysis program to produce individual force versus z-lift curves (see Supplementary Fig. 1) according to protocols described by Jalilian et al. (2015). Height was estimated as the mean *z*-lift value for each scan relative to the length of the scan. YM was estimated by the Nanoscope Analysis program from the slope of the force curves using Sneddon's model (Sneddon, 1965), following Roa et al. (2011) and Offroy et al. (2020). Mean roughness was estimated as the sum of the mean value of the five tallest *z*-lift peaks and the five deepest *z*-lift valleys across the entirety of each scan (Hansma and Hoh, 1994; Müller and Anderson, 2002).

The reliability of our estimates was checked by comparing our YM values with those previously attained for *A. keyserlingi* and *L. hasselti* MA silk fibres (Blamires et al., 2016, 2018). Full scans were repeated for each sample at four randomly chosen locations along the silk thread. We accordingly were confident that any variability in height and/or YM measured between the protein deprived and protein fed spider's silks were not influenced by the feedback signal transmitted to the piezo (Chlanda et al., 2015). The parameters measured were manually recorded upon completing each scan and entered into a Microsoft Excel database to facilitate the following statistical analyses.

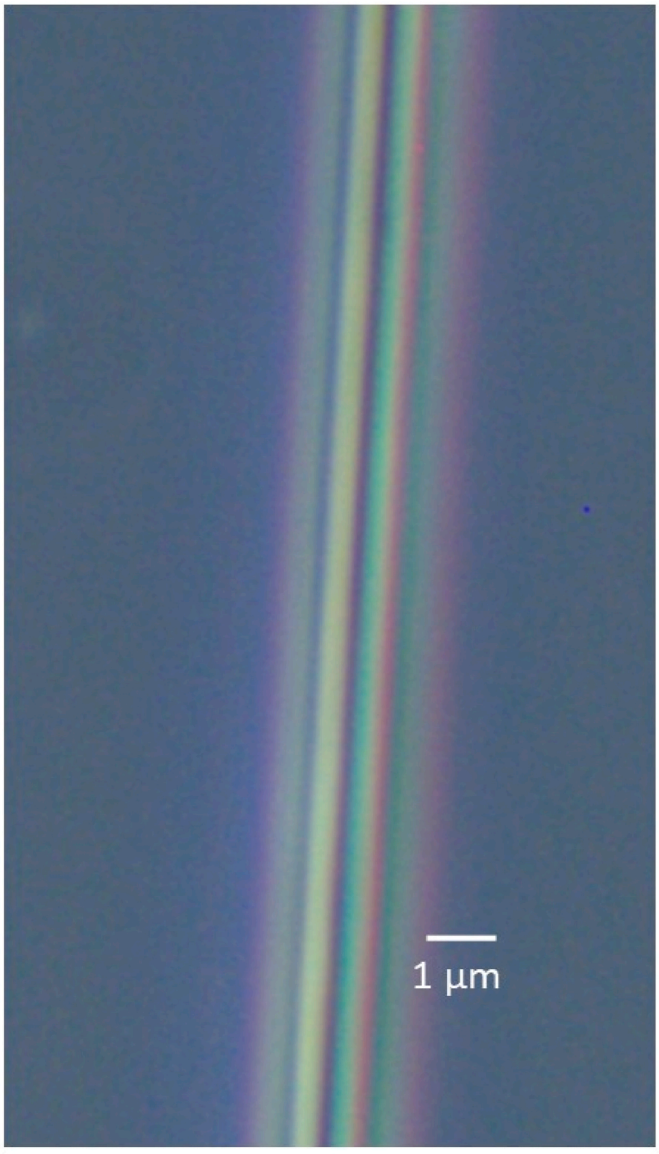

Fig. 1. Example of a silk fibre (*A. keyserlingi*) imaged using the optical microscope. Note the two silk fibres aligned side-by-side.

2.4. Statistical comparisons of parameters

We combined the measurements made at each of the four locations for each silk sample to attain mean parameter values for each scan. We considered these mean values as individual across treatment replicates for the subsequent one-way (factor = treatment) multivariate analyses of variance (MANOVAs) comparing height and YM between silks from protein deprived and protein fed spiders.

We performed separate MANOVAs each for *A. keyserlingi* and *L. hasselti* silks. Whenever these multivariate analyses found a significant difference between treatments we performed individual one-way analyses of variance (ANOVAs) on each response variable to ascertain the variables that significantly differed across the treatments. We performed the data analyses upon *a priori* checking for normality and homoscedasticity using Q-Q plots and residual distributions using the R suite of packages.

3. Results and discussion

Our MANOVAs found protein deprivation to affect overall MA silk properties (see Supplementary Table 1). Individual one-way analyses of variance for each parameter identified height and YM as differing between the silks of protein deprived and protein fed *A. keyserlingi* (Supplementary Table 1, Fig. 2).

Variations in height and modulus have been reliably ascribed to core and surface nano-scale variations in proteins and other substances whose structural composition were known *a priori* (Magonov et al., 1997; Melitz et al., 2011). Our findings thus imply that the nutritional state of *A. keyserlingi* and *L. hasselti* results in variations in their silk's core and skin thickness, composition and topography. We thereupon drew the following conclusions about the probable consequences of these variations on bulk fibres using published information about their: (i) spidroin expressions, (ii) crystalline and non-crystalline nano features, and (iii) bulk mechanics, across identical dietary manipulations (Blamires et al., 2018).

Thread heights were herein estimated from peak cantilever *z*-lift values and is an estimate of the thread diameters at specific points across the surface. We accordingly predicted that all of the silk threads had widths of between 1 μm and 2 μm, with *A. keyserlingi*'s threads being consistently wider than those of *L. hasselti*. Although the silks of both species varied in height across feeding treatments, the differences were not as substantive between treatments for *L. hasselti*'s silk as they were for *A. keyserlingi*'s silk (Fig. 2A). Upon checking the mean roughness estimates (Fig. 3; one-way analyses of variances: $p > 0.05$) we found no evidence that this might be an artifact of surface roughness differing

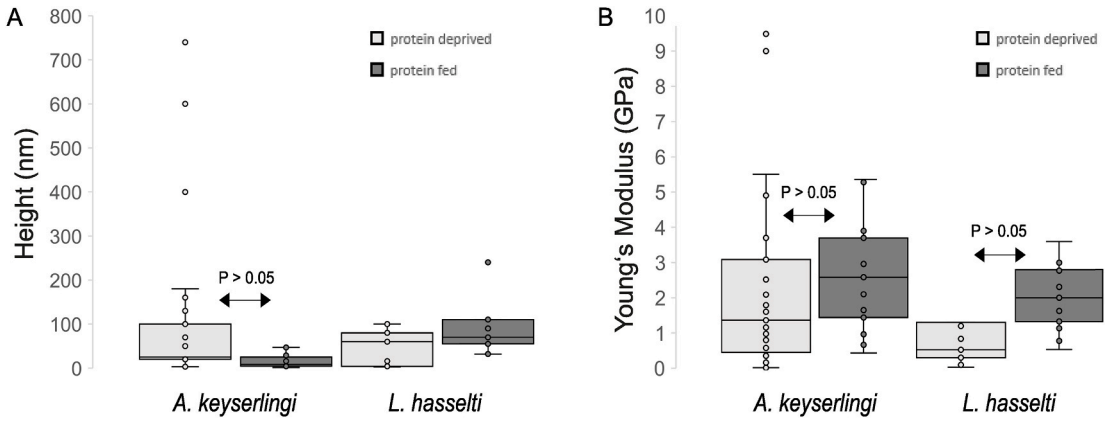

Fig. 2. Box-plots comparing: (A) height, and (B) Young's modulus (YM) between the silks of protein deprived and protein fed *A. keyserlingi* and *L. hasselti*. Plots display the median (line), 25% quartiles (boxes), extremities (whiskers), and outliers (peripheral dots). Significant differences between mean values are indicated (full statistics are in Supplementary Table 1).

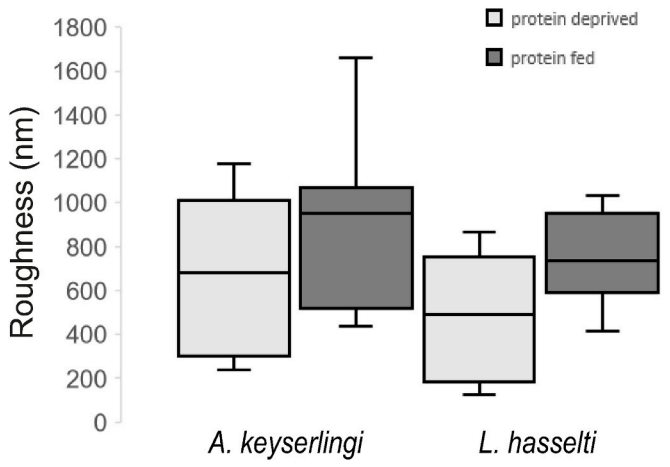

Fig. 3. Comparison of roughness values (nm) of *A. keyserlingi* and *L. hasselti* silks across protein fed and protein deprived treatments. Plots display the median (line), 25% quartiles (boxes), extremities (whiskers). One-way analyses of variances found no between treatment differences in the mean values for either species.

across individual silks when spiders were protein fed or deprived.

We found substantially greater variability in YM values for *A. keyserlingi*'s silk across treatments than for *L. hasselti*'s silk (Fig. 2B), meaning that these spiders would have built webs that varied in their capacity to capture prey. Dynamic modelling experiments, such as those conducted by Harmer et al. (2015) and Blamires and Sellers (2019), are a useful way to determine whether this manifests as an impairment or enhancement of web performance. Such experiments were beyond the intended scope of this study, but could be incorporated into future studies aiming to ascertain the ecological consequences of multi-scales variations in spider silk mechanical performance.

There is evidence that a range of unusual topographic features, e.g. torsions, voids, or bundling, affect the width, and subsequent performance, of spider silk (Augsten et al., 2000; Liu et al., 2019). Our optical microscopy (see Fig. 1 for a representation) and topographic imaging (Fig. 4) failed to detect any voids, bundles or twists, or any other kind of modification in any of the fibres, and all heights measured were well in the *z*-range detectable by the piezo of the Atomic Force Microscope. It thus seems unlikely that any large attachments, bundles, or twists went undetected. Nevertheless, with the scan size in the X and Y set at 10 μm, we may have scanned around any large bundles or twists. Notwithstanding, we expect that such bundles and twists would have been visible with the naked eye and/or under the optical microscope and subsequently avoided. An alternative explanation for the interspecific variability in height was that some images may have been performed within a void. Considering the general smoothness of MA silk reported here and elsewhere (Li et al., 1994; Silva and Rech, 2013; Yazawa et al., 2018), we regard this as highly unlikely.

The height measurements for each of the two species' silks was highly variable. Other AFM experiments of spider MA silk (e.g. Gould et al., 1999; Oroudjev et al., 2002; Menezes et al., 2013; Silva and Rech, 2013) have reported a similar wide range of height measurements among differing species. We are therefore confident that the ranges of roughness (see Fig. 3) and height (see Fig. 4) values measured herein are reliable and consistent with those made previously for the MA silks of other *Argiope* and *Latrodectus* species of (e.g. mean height ~1.0 μm and roughness ~400 nm for *A. keyserlingi*; Kane et al., 2010, and height: ~2.0 μm for *L. hesperus*; Gould et al., 1999).

AFM studies of large proteins (Hughes and Dougan, 2016), including those for spider silks (Li et al., 1994; Kane et al., 2010; Menezes et al., 2013; Wang and Schniepp, 2018), have shown height values measured using AFM can be used to interpret the presence of nano structural features such β-sheets density, and the interspersion of helical structures, across the skin and core. Considering this, we are confident in ascribing the differences in height that our topographies suggest across species and treatments as a consequence of spinning processes inducing differential structure formations such as the formation of β –sheets from β –turns and other secondary structures (Augsten et al., 2000; Yazawa et al., 2018).

We determined YM here to compare localized stiffness of the threads along the silk fibre surface between species and treatments. We subsequently found it to differ across treatments for both *L. hasselti*'s and *A. keyserlingi*'s MA silks (Fig. 2B), albeit with *A. keyserlingi*'s silk affected to a greater extent than *L. hasselti*'s. This accordingly enabled us to also conclude that protein deprivation induces, in both species, nanoscale mechanical and structural property changes of the silk's skin and core.

The same feeding treatments as those used here have been used to induce significant changes in crystallinity within the core proteins of *A. keyserlingi*'s MA silk, with subsequent effects on bulk mechanics (Blamires et al., 2018). However, no nutritionally induced core protein or bulk mechanical variations have been found for *L. hasselti*'s MA silk (Blamires et al., 2018). We, likewise, found that height and YM varied across treatment in *A. keyserlingi*'s silk and concluded that the across treatments changes in their skin-core structures corresponded with nanoscale mechanics that scale to bulk properties. For L. *hasselti*'s silk, however, localized stiffness varied significantly across treatments, as signified by the YM variations found, while height marginally differed across treatments. These findings suggest that *L. hasselti*'s silk has some

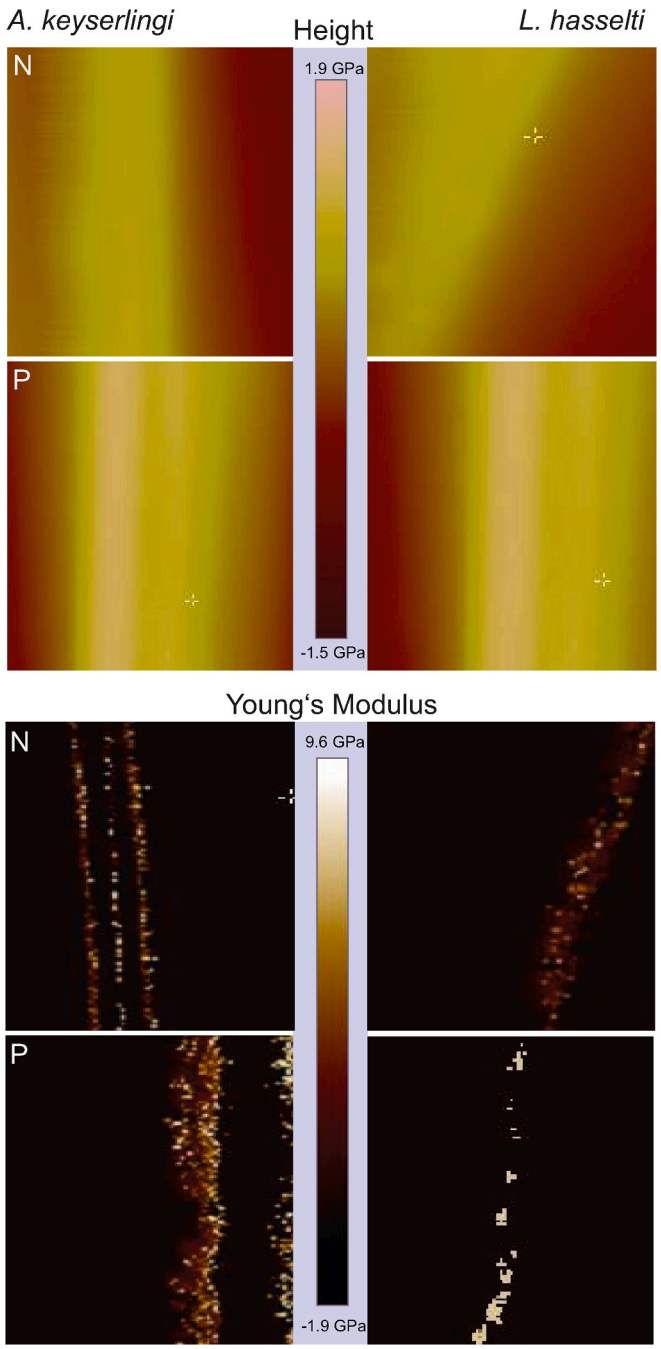

Fig. 4. Example Peak Force Quantitative Nanomechanical (QNM) topography profiles of protein deprived (N) and protein fed (P) *A. keyserlingi* and *L. hasselti* MA silk, showing the results derived by Nanoscope Analysis for height (mean *z*-lift value) and (DMT) modulus. The N and P representative images for each species are not for the same fibre sample, thus the measurement peaks appear in different locations in each instance.

degree of nanoscale structural variability that does not manifest as variations in its bulk properties. We thus expect that other features within the skin and/or core, such as multi-level intralaminar features (Colomban and Dinh, 2012), facilitate the decoupling observed between structure and function and bulk fibre properties in *L. hasselti*'s MA silk.

4. Conclusions

Previous studies have shown that protein structures and mechanical properties vary in the MA silks of *Argiope* spp. as the spider's protein intake varies. Such variations in properties and structures have not been detected for the MA silks of *Latrodectus* spiders. Here we used AFM to simultaneously ascertain the topographic, structural, and mechanical properties of the MA silks of *A. keyserlingi* and *L. hasselti* at the nanoscale to determine whether they varied in property across protein intake in a similar manner to bulk fibres.

We found significant across species and treatment differences in localized fibre diameter and stiffness. We ascribe these to the skin-core structures of the MA silk of both species varying in composition under different feeding treatments. Furthermore, we expect that these variations have been induced by changes to the expressed ratio of MaSp1: MaSp2 (as suggested by Blamires et al., 2018). The structures varied most substantially across treatment in *A. keyserlingi*'s silk, but some degree of variability was detected in *L. hasselti*'s silk. This was surprising, as we predicted the nanoscale structure and function variations in each species' silk to correspond with their bulk properties. We speculated that the decoupling of the structure-function relationship evident when determining the bulk properties of *L. hasselti*'s fibres is a consequence of variations in the intralaminar features.

Our findings overall suggest that nutritional status of the spider affects silk nanostructures, with subsequent influences on localized properties. The manifestation of these effects differs across species and scales and is important to understand and consider when devising genetic engineering or biomimetic spinning programs.

CRediT authorship contribution statement

Sean J. Blamires: Conceptualization, Data curation, Formal analysis, Funding acquisition, Project administration, Methodology, Resources, Writing – review & editing, Investigation, Writing – original draft, Validation. **Madeleine Nobbs:** Data curation, Investigation, Resources, Writing – original draft. **Jonas O. Wolff:** Formal analysis, Writing – original draft, Validation, Methodology, Investigation, Funding acquisition. **Celine Heu:** Data curation, Formal analysis, Methodology, Resources, Software, Validation, Writing – original draft.

Declaration of competing interest

The authors declare the following financial interests/personal relationships which may be considered as potential competing interests: Sean Blamires reports administrative support and equipment, drugs, or supplies were provided by University of New South Wales. Sean Blamires reports financial support was provided by Hermon Slade Foundation. Sean Blamires reports a relationship with University of New South Wales that includes: employment.

Acknowledgements

S.J.B. received financial support from the Australian Research Council (DE140101281) and Hermon Slade Foundation (HSF17/6). J.O. W. was supported by a Discovery Early Career Researcher Award from the Australian Research Council (DE190101338).

Appendix A. Supplementary data

Supplementary data to this article can be found online at https://doi.org/10.1016/j.jmbbm.2021.104873.

References

Augsten, K., Muhlig, P., Hermann, C., 2000. Glycoproteins and skin-core structure in *Nephila clavipes* spider silk observed by light and electron microscopy. Scanning 22, 12–15.

Bhushan, B., Koinkar, V.N., 1994. Nanoindentation hardness measurements using atomic force microscopy. Appl. Phys. Lett. 64, 1653–1655.

Blamires, S.J., Blackledge, T.A., Tso, I.M., 2017. Physico-chemical property variation in spider silks: ecology, evolution and synthetic production. Annu. Rev. Entomol. 62, 443–460.
Blamires, S.J., Kasumovic, M.M., Tso, I.M., Martens, P.J., Hook, J.M., Rawal, A., 2016. Evidence of decoupling of spidroin expression and protein structure in spider dragline silks. Int. J. Mol. Sci. 17, 1294.
Blamires, S.J., Liao, C.P., Chang, C.K., Chuang, Y.C., Wu, C.L., Blackledge, T.A., Sheu, H. S., Tso, I.M., 2015. Mechanical performance of spider silk is robust to nutrient-mediated changes in protein composition. Biomacromolecules 16, 1218–1225.
Blamires, S.J., Nobbs, M., Martens, P.J., Tso, I.M., Chuang, W.S., Chang, C.K., Sheu, H.S., 2018. Multiscale mechanisms of nutritionally-induced property variation in spider silk. PLoS One 213, e0192005.
Blamires, S.J., Sellers, W.I., 2019. Modelling temperature and humidity effects on web performance: implications for predicting orb-web spider (*Argiope* spp.) foraging under Australian climate change scenarios. Cons. Physiol. 7, coz083.
Blamires, S.J., Wu, C.C., Wu, C.L., Sheu, S.H., Tso, I.M., 2013. Uncovering spider silk nanocrystalline variations that facilitate wind- induced mechanical property changes. Biomacromolecules 14, 3484–3490.
Boutry, C., Blackledge, T.A., 2013. Wet webs work better: humidity, supercontraction and the performance of spider orb webs. J. Exp. Biol. 216, 3606–3610.
Bratzel, G., Buehler, M.J., 2011. Molecular mechanics of silk nanostructures under varied mechanical loading. Biopolymers 97, 408–417.
Chlanda, A., Rebis, J., Kijenska, E., Wozniak, M.J., Rozniatowski, K., Swieszkowski, W., Kurzydlowski, K.J., 2015. Quantitative imaging of electrospun fibers by Peak Force Quantitative Nano Mechanics atomic force microscopy using etched scanning probes. Micron 72, 1–7.
Colomban, P., Dinh, H.M., 2012. Origin of the variability of the mechanical properties of silk fibres: 2 the nanomechanics of single silkworm and spider fibres. J. Raman Spectrosc. 43, 1035–1041.
Craig, H.C., Blamires, S.J., Sani, M.A., Kasumovic, M.M., Rawal, A., Hook, J.M., 2019. DNP NMR spectroscopy reveals new structures, residues and interactions in wild spider silks. Chem. Comms. 55, 4687–4690.
Craig, H.C., Piorkowski, D., Nakagawa, S., Kasumovic, M.M., Blamires, S.J., 2020. Meta-analysis reveals materiomic relationships in major ampullate silk across the spider phylogeny. J. Roy. Soc. Interf. 17, 20200471.
Du, N., Yang, Z., Liu, Y., Li, Y., Xu, H.Y., 2011. Structural origin of the strain-hardening of spider silk. Adv. Funct. Mater. 21, 772–778.
Eisoldt, L., Hardy, J.G., Heim, M., Scheibel, T.R., 2010. The role of salt and shear on the storage and assembly of spider silk proteins. J. Struct. Biol. 170, 413–419.
Garcia, R., 2020. Nanomaterial mapping of soft materials with the atomic force microscope: methods, theory and applications. Chem. Soc. Rev. 49, 5850–5884.
Gomes, S., Numata, K., Leonor, I., Mano, J.F., Reis, R.L., Kapaln, D.L., 2011. AFM study of morphology and mechanical properties of a chimeric spider silk and bone sialoprotein protein for bone regeneration. Biomacromolecules 12, 1675–1685.
Gould, S.A.C., Tran, K.T., Spagna, J.C., Moore, A.M.F., Shulman, J.B., 1999. Short and long range order of the morphology of silk from *Latrodectus hesperus* (Black Widow) as characterized by atomic force microscopy. Int. J. Biol. Macromol. 24, 151–157.
Guan, J., Porter, D., Vollrath, F., 2013. Thermally induced changes in dynamic mechanical properties of native silks. Biomacromolecules 14, 930–937.
Guo, C., Zhang, J., Jordan, J.S., Wang, X., Henning, R.W., Yarger, J.L., 2018. Structural comparison of various silkworm silks: an insight into the structure−property relationship. Biomacromolecules 19, 906–917.
Hansma, H.G., Hoh, J.H., 1994. Biomolecular imaging with the atomic force microscope. Annu. Rev. Biophys. Biomol. Struct. 23, 115–139.
Harmer, A.M.T., Clausen, P.T., Wroe, S., Madin, J.S., 2015. Large orb-webs adapted to maximise total biomass not rare, large prey. Sci. Rep. 5, 14121.
Heu, C., Berquand, A., Elie-Caille, C., Nicod, L., 2012. Glyphosate-induced stiffening of HaCaT keratinocytes, a Peak Force Tapping study on living cells. J. Struct. Biol. 178, 1–7.
Hudspeth, M., Nie, X., Chen, W., Lewis, R.V., 2012. Effect of loading rate on mechanical properties and fracture morphology of spider silk. Biomacromolecules 13, 2240–2246.
Hughes, L., Dougan, L., 2016. The physics of pulling polyproteins: a review of single molecule force spectroscopy using the AFM to study protein unfolding. Rep. Prog. Phys. 79, 076601.
Jalilian, I., Heu, C., Cheng, H., Feittag, H., Desouza, M., Stehn, J.R., Bryce, N.S., Whan, R. M., Hardeman, E.C., Fath, T., Schevzov, G., Gunning, P.W., 2015. Cell elasticity is regulated by the tropomyosin isoform composition of the actin cytoskeleton. PLoS One 10, e0126214.
Kane, D.M., Naidoo, N., Staib, G.R., 2010. Atomic force microscopy of orb-spider-web-silks to measure surface nanostructuring and evaluate silk fibers per strand. J. Appl. Phys. 108, 073509.
Kohler, T., Vollrath, F., 1995. Thread biomechanics in the two orb-weaving *spiders Araneus diadematus* (Araneae, Araneidae) and *Uloborus walckenaerius* (Araneae, Uloboridae). J. Exp. Zool. 271, 1–17.
Li, S.F.Y., McGhie, A.J., Tang, S.L., 1994. New internal structure of spider dragline silk revealed by atomic force microscopy. Biophys. J. 66, 1209–1212.
Lin, L.H., Edmonds, D.T., Vollrath, F., 1995. Structural engineering of an orb spiders web. Nature 373, 146–148.
Lin, S., Ryu, S., Torekeva, O., Gronau, G., Jacobsen, M.M., Rizzo, D.J., Li, D., Staii, C., Pugno, N.M., Wong, J.Y., Kaplan, D.L., Beuhler, M.J., 2015. Predictive modelling-based design and experiments for synthesis and spinning of bioinspired silk fibres. Nat. Commun. 6, 6892.
Lintz, E.S., Scheibel, T.R., 2013. Dragline, egg stalk and byssus: a comparison of outstanding protein fibers and their potential for developing new materials. Adv. Funct. Mater. 23, 4467–4482.
Liu, D., Tarakanova, A., Hsu, C.C., Yu, M., Yu, L., Liu, J., He, Y., Dunstan, D.J., Beuhler, M.J., 2019. Spider dragline silk as torsional actuator driven by humidity. Sci. Adv. 5, eaau9183.
Liu, Y., Shao, Z.Z., Vollrath, F., 2005. Relationships between supercontraction and mechanical properties of spider silk. Nat. Mater. 4, 901–905.
Melitz, W., Shen, J., Kummel, A.C., Lee, S., 2011. Kelvin probe force microscopy and its application. Surf. Sci. Rep. 66, 1–27.
Menezes, G.M., Teulé, F., Lewis, R.V., Silva, L.P., Rech, E.L., 2013. Nanoscale investigations of synthetic spider silk fibers modified by physical and chemical processes. Polym. J. 45, 997–1006.
Magonov, S.N., Elings, V., Whangbo, M.H., 1997. Phase imaging and stiffness in tapping-mode atomic force microscopy. Surf. Sci. 375, L385–L391.
Müller, D.J., Anderson, K., 2002. Biomolecular imaging using atomic force microscopy. Trends Biotechnol. 20, S45–S49.
Neubauer, M.P., Blüm, C., Agostini, E., Engert, J., Scheibel, T.R., Fery, A., 2013. Micromechanical characterization of spider silk particles. Biomater. Sci. 1, 1160–1165.
Offroy, M., Razafitianamaharavo, A., Beaussart, A., Pagnout, C., Duval, J.F., 2020. Fast automated processing of AFM peakforce curves to evaluate spatially resolved Young's modulus and stiffness of turgescent cells. RSC Adv. 10, 19258–19275.
Oroudjev, E., Soares, J., Thompson, J.B., Fossey, S.A., Hansma, H.G., 2002. Segmented nanofibres of spider dragline silk: atomic force microscopy and single-molecule force microscopy. Proc. Natl. Acad. Sci. Unit. States Am. 99, 6460–6465.
Papadopoulos, P., Solter, J., Kramer, F., 2009. Similarities in the structural organization of major and minor ampullate spider silk. Macromol. Rapid Comms. 30, 851–857.
Paquet-Mercier, F., Lefevre, T., Auger, M., Pezolet, M., 2013. Evidence by infrared spectroscopy of the presence of two types of β-sheets in major ampullate spider silk and silkworm silk. Soft Matter 9, 208–215.
Parkhe, A.D., Seeley, A.K., Gardner, K., Thompson, L., Lewis, R.V., 1997. Structural studies of spider silk proteins in the fiber. J. Mol. Recogn. 10, 1–6.
Patil, S.P., Markert, B., Grater, F., 2014. Rate-dependent behavior of the amorphous phase of spider dragline silk. Biophys. J. 106, 2511–2518.
Piorkowski, D., He, B.C., Blamires, S.J., Tso, I.M., Kane, D.M., 2021. Nanoscale material heterogeneity of glowworm capture threads revealed by AFM. Molecules 26, 3500.
Roa, J.J., Oncins, J., Diaz, J., Sanz, F., Segarra, M., 2011. Calculation of Young's modulus value by means of AFM. Rec. Pat. Nanotech. 5, 27–36.
Sensenig, A.T., Lorentz, K.A., Kelley, S.P., Blackledge, T.A., 2012. Spider orb webs rely on radial threads to absorb prey kinetic energy. J. Roy. Soc. Interf. 9, 1880–1891.
Silva, L.P., Rech, E.L., 2013. Unravelling the biodiversity of nanoscale signatures of spider silk fibres. Nat. Commun. 4, 3014.
Sneddon, I.N., 1965. The relation between load and penetration in the axisymmetric boussinesq problem for a punch of arbitrary profile. Int. J. Eng. Sci. 3, 47–57.
Tarakanova, A., Buehler, M.J., 2012. The role of capture spiral silk properties in the diversification of orb webs. J. Occup. Med. 64, 214–225.
Wang, Q., Schniepp, H.C., 2018. Strength of recluse spider's silk originates from nanofibrils. ACS Macro Lett. 7, 1364–1370.
Wolff, J.O., Wells, D., Reid, C.R., Blamires, S.J., 2017. Clarity of objectives and working principles enhances the success of biomimetic programs. Bioinspiration Biomimetics 12, 051001.
Yazawa, K., Malay, A.D., Maunaga, H., Numata, K., 2018. Role of skin layers on mechanical properties and supercontraction of spider dragline silk fiber. Macromol. Biosci. 18, 1800220.
Zhang, W., Xu, Q., Zou, S., Li, H., Xu, W., Zhang, X., 2000. Single-molecule force spectroscopy on *Bombyx mori* silk fibroin by Atomic Force Microscopy. Langmuir 16, 4305–4308.